Measurement ranges of these assays were 5 to 5000 KIU/mL and 1.2 to 7.8 log IU, respectively.

Liver Biopsy

Liver biopsy specimens were evaluated by a pathologist at each institution and were scored for the stage of liver fibrosis according to the classification of Desmet et al.[12] Stage of fibrosis was assessed from stage F0 (no fibrosis) to stage F4 (cirrhosis). The patients were divided into 2 categories: mild fibrosis (F0−1) and severe fibrosis (F2−4).

ITPA Expression

Total RNA was extracted from white blood cell samples of HCV patients using RNeasy Mini Kit (Qiagen, Hilden, Germany) and reverse-transcribed using ReverTra Ace (TOYOBO, Osaka, Japan) with random primers according to manufacturer's instructions. We then amplified complementary DNAs by 35 cycles of PCR in a 25-mL reaction volume containing 1× KOD-Plus buffer (0.3 mM each primer, 0.2 mM $MgSO_4$, 1 mL DNA solution, and 1 U KOD-Plus [TOYOBO Co.]). The thermal profile was initial denaturation at 98°C for 2 minutes, followed by 35 cycles of amplification (denaturation at 98°C for 15 seconds, annealing at 58°C for 15 seconds, and extension at 68°C for 60 seconds). Nucleotide sequences of the amplified complementary DNA fragments were confirmed by direct sequencing. Real-time quantitative PCR was performed employing an ABI PRISM 7100 (Applied Biosystems) with the SYBR Green PCR Master Mix Kit (Applied Biosystems) according to manufacturer's instructions. The housekeeping gene glyceraldehyde-3-phosphate dehydrogenase was used as an internal standard.

Statistical Analysis

After GWAS-1 quality control, a linear regression model was used to test for an association between SNP genotype and Hb decline, where an additive effect of genotype was assumed. The inflation factor was estimated by the genomic control method. Multivariate logistic regression analysis with stepwise forward selection was performed with $P < .05$ as the criteria for model inclusion using the StatFlex 5.0 software package (Artec Inc, Osaka, Japan).

Results

Genome-Wide Association Analysis and Replication Study

A total of 510,537 SNPs passed quality-control filters. During the quality-control check, 11 samples suggesting kinship or sample duplication were excluded from the analysis according to PI_HAT value. The threshold for genome-wide significant association was set at $P < 9.8 \times 10^{-8}$ (.05/510,537). The genomic distribution of SNP associations is shown in Supplementary Figure

Table 2. Genome-Wide Association Study of Hemoglobin Decline at Week 4

	Set	GWAS 1			GWAS 2			Replication 1			Combined		
	Genotype	CC	CA	AA	CC	CA	AA	CC	CA	AA	CC	CA	AA
rs6051639[a] (C/A)[b]	n	108	229	116	44	111	57	68	117	73	220	457	246
	Hb decline at 4 week, g/dl	−2.48 (1.64)	−1.91 (1.44)	−1.49 (1.38)	−2.44 (1.63)	−2.10 (1.52)	−1.34 (1.64)	−2.39 (1.76)	−1.81 (1.57)	−1.31 (1.35)	−2.48 (1.63)	−1.95 (1.48)	−1.43 (1.44)
	P value[a]		4.5×10^{-7}			1.5×10^{-4}			2.0×10^{-5}			6.0×10^{-14}	
	r[c]		0.24			0.26			0.26			0.24	
rs1127354[a] (C/A)[b]	n	337	108	8	164	43	5	192	62	4	693	213	17
	Hb decline at 4 week, g/dl	−2.40 (1.45)	−0.80 (0.87)	0.20 (1.38)	−2.39 (1.48)	−0.69 (1.32)	0.07 (0.95)	−2.22 (1.62)	−0.73 (0.93)	−0.10 (1.18)	−2.34 (1.50)	−0.78 (0.99)	−0.19 (1.12)
	P value[a]		7.5×10^{-26}			2.2×10^{-11}			5.6×10^{-11}			3.5×10^{-44}	
	r[c]		0.47			0.44			0.39			0.44	

NOTE. Data given for continuous variables are mean (standard deviation) unless otherwise stated.
[a]*P* value by linear regression testing.
[b]Pearson's correlation coefficient representing the effect of a minor allele on the trait.
[c](Major/minor) allele in Japanese population.
[d]The top single nucleotide polymorphism in the genome-wide association study (GWAS) screening.
[e]Missense variant in the inosine triphosphate pyrophosphatase gene.

1A. The quantile−quantile plot demonstrated that several SNPs showed a stronger association than would be expected by chance, but were not significant (Supplementary Figure 1B), with a genomic inflation factor of 1.005. SNPs with $1.6 \times 10^{-7} \leq P < 1.0 < 10^{-5}$ were considered suggestive and retained for follow-up in the second stage. Of 49 SNPs taken forward into GWAS-2, only 1 SNP, rs6051639, located in the DDRGK1 gene on chromosome 20 (20p13 region), was found to be strongly associated with treatment-induced Hb reduction, based on the Bonferroni threshold by replication method. This association was validated in Replication-1 (Table 2).

Resequencing and Fine-Mapping

We resequenced the region surrounding the top SNP rs6051639 associated with treatment-related anemia. A recent study has reported that a missense variant in the ITPA gene affects ribavirin-induced anemia.[8] ITPA and DDRGK1 are adjacent on chromosome 20; therefore, although the LD block spans about 3 kb (Figure 1), we resequenced an approximately 37-kb genomic region encompassing DDRGK1 and ITPA loci and identified 83 common variants with minor allele frequency >0.05, 6 of which were novel (Supplementary Table 1). Of these, we genotyped as many nonredundant SNPs as possible. Four SNPs, including rs1127354, were significantly associated with ribavirin-induced anemia and in almost absolute LD with each other (Figure 1). The combined analyses of the screening and replication studies demonstrated a highly significant combined *P* value for rs1127354 (Table 2). In contrast to the considerable association found for Hb decline, baseline Hb level was not correlated with SNP (Figure 2). A significantly larger proportion of patients with the rs1127354 A allele completed treatment without ribavirin dose reduction compared to those homozygous

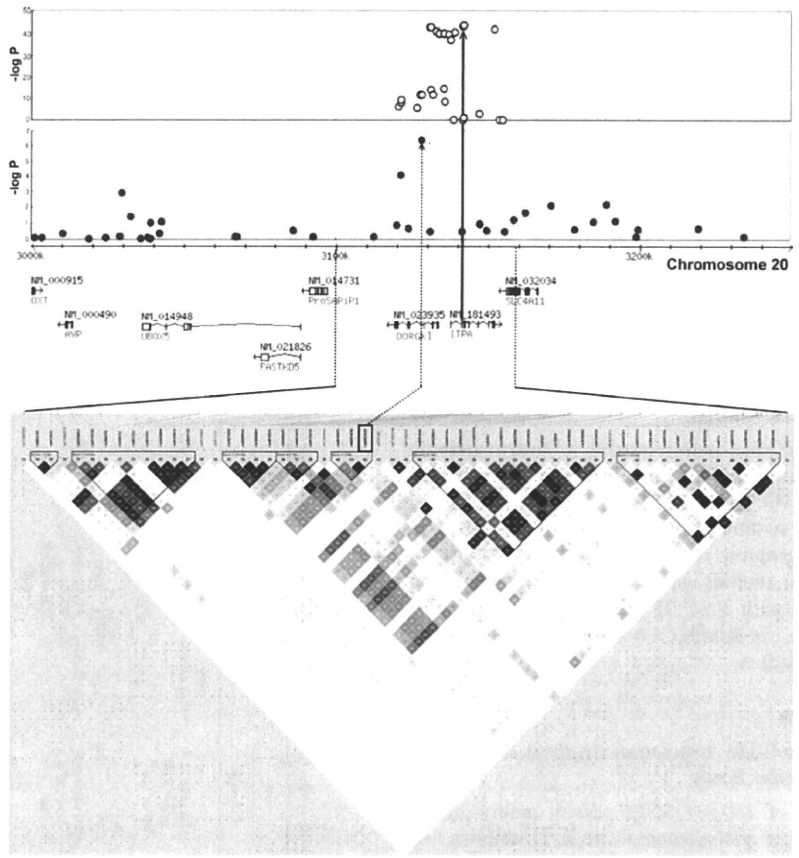

Figure 1. Depiction of the haplotype structure around the top locus. *P* value plots in linear regression analysis in genome-wide association study (GWAS)-1 stage (*middle panel*), fine-mapping using GWAS-1, GWAS-2, and Replication-1 samples (*upper panel*), and linkage disequilibrium (LD) map around DDRGK1 and inosine triphosphate pyrophosphatase (ITPA) using HapMap JPT datasets. *Dark gray*: regions with high r^2 values, *light gray*: regions with low r^2 values (*lower panel*). *Dashed line* and *arrow* represent the top single nucleotide polymorphism (SNP) rs6051639 identified by GWAS. The *solid line* and *arrow* represent the missense variant rs1127354 in the *ITPA* gene.

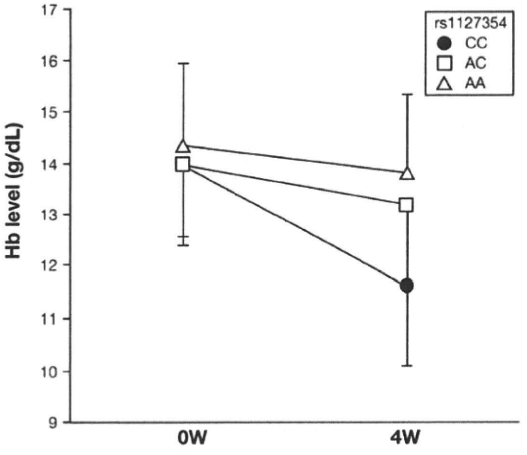

Figure 2. Inosine triphosphate pyrophosphatase (ITPA) variants and hemoglobin (Hb) level at baseline and 4-week. All the samples enrolled in the present study were stratified based on rs1127354 genotype. Markers represent means and each error bar represents 1 standard deviation.

for the C allele (rs1127354 AA/CA (83%) vs CC (37%); $P < .01$), suggesting that the A allele is protective.

ITPA Expression Level and Ribavirin-Induced Hb Decline

Real-time quantitative PCR assays revealed no correlation between ITPA expression level and ribavirin-induced Hb decline in white blood cells. Even in stratified analysis based on the missense SNP rs1127354 genotype, we still found no correlation (Figure 3). Furthermore, we evaluated the association between ITPA expression for each SNP in the block we genotyped and found no SNPs associated with ITPA expression (data not shown).

Variables Associated With Severe Anemia

To examine the influence of potentially important prognostic factors on severe anemia (Hb <10 g/dL) necessitating dose reduction or drug withdrawal, 5 factors including known risk factors (age, sex, baseline Hb level, baseline platelet count, and rs1127354) were first examined individually by univariate logistic regression on each factor for 893 patients from the GWAS-1, GWAS-2, and Replication-1 groups. These factors were clearly associated with severe anemia (Table 3). To assess the independence of these factors, stepwise forward multiple logistic regression analysis was performed. Except for sex, all variables that were significant under univariate analyses remained significant in the final multivariate model (Table 3).

Variables Associated With Treatment Outcomes

To evaluate whether the ITPA variant affects treatment outcomes, logistic regression was used to analyze data from 522 patients who completed the therapy program with >75% compliance with prescribed doses of PEG-IFN and ribavirin. Patients were classified into the following 2 groups based on treatment outcomes: sustained viral responder and nonresponder. Sustained viral responders had no evidence of viremia at 24 weeks after completion of interferon therapy, whereas nonresponders remained viremic at this stage.

Initially 9 factors, including age, sex, BMI, baseline Hb level, baseline platelet count, fibrosis, baseline viral titer, rs1127354, and a recently reported IL-28B variant (rs8099917) genetic risk factor,[13,14] were examined individually by univariate logistic regression analysis. Individually these factors were each significantly associated with treatment outcome (Table 4). To identify independent factors, stepwise forward multiple logistic regression analysis was performed, and all variables identified by univariate analyses were retained in the final multivariate model except for baseline hemoglobin level. ITPA variant rs1127354 was retained in the final model but showed no significant association ($P = .10$) (Table 4).

Discussion

The anemia experienced as a consequence of PEG-IFN and ribavirin combination therapy is primarily caused by a ribavirin-induced hemolysis and secondarily by an interferon-induced bone marrow toxicity. De

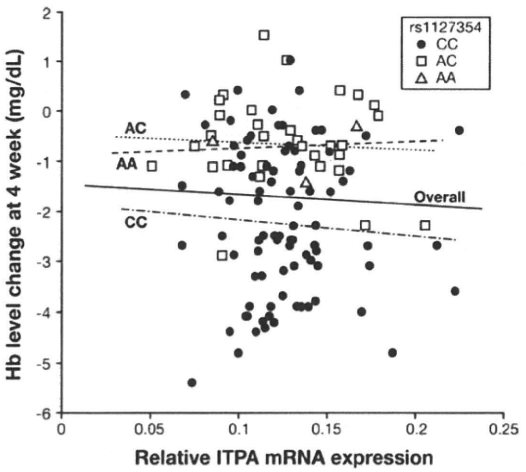

Figure 3. Inosine triphosphate pyrophosphatase (ITPA) expression level and ribavirin-induced anemia. Among genome-wide association study (GWAS)-1 and GWAS-2 patients, 124 white blood cell samples were collected and analyzed. The y-axis represents hemoglobin (Hb) level change at week 4 compared with baseline, and the x-axis represents relative messenger RNA (mRNA) expression levels of ITPA standardized by glyceraldehyde-3-phosphate dehydrogenase. The *thick solid line* represents the overall least squares best fit line and the *other 3 lines* represent best fit stratified by missense single-nucleotide polymorphism rs1127354 genotypes.

Table 3. Predictive Factors for Ribavirin-Induced Anemia in Hepatitis C Virus Patients Determined by Multivariate Logistic Regression Analysis

Variable	*P* (univariate)	*P* (multivariate)	OR	95% CI
rs1127354 (C/A)[a]	4.6×10^{-4}	1.3×10^{-4}[b]	0.20[c]	0.092–0.46
Age	.00012	.06	1.03[d]	1.00–1.05
Sex	.0065	—		
Baseline platelet count	1.0×10^{-6}	.015	0.92[e]	0.87–0.97
Baseline Hb level (*g/dL*)	2.4×10^{-14}	2.4×10^{-11}	0.56[f]	0.48–0.67

CI, confidence interval; Hb, hemoglobin; OR, odds ratio.
[a](Major/minor) allele.
[b]Additive model.
[c]The per-minor allele OR for ribavirin-induced anemia.
[d]Per year increase.
[e]Per 10^4 platelet count increase.
[f]Per g/dL hemoglobin increase.

Franceschi et al[15] proposed that the mechanism of ribavirin toxicity is that ribavirin phosphate accumulation in erythrocytes mediates oxidative damage and cell lysis. It has been reported that anemia is the major reason for dose reduction.[16] Various predictive factors for ribavirin-induced anemia have been proposed,[4–7] but it nonetheless remains difficult to predict the risk of hemolysis before administration of the drug. Haptoglobin phenotype[6] may be recognized as one of the genetic variants associated with ribavirin-induced hemolysis, although the underlying molecular mechanisms are still unknown. Recently, Fellay et al found 2 ITPA functional SNPs showing strong independent association with treatment-induced hemoglobin reduction by genome-wide association analysis.[8] Our study also identified the same missense variant in the Japanese population through genome-wide scanning followed by fine-mapping. In contrast to Fellay et al's findings, however, the splicing variant SNP rs7270101 was monoallelic in the Japanese population, and there appeared to be no other causal variants or synthetic associations with ITPA. Similarly, we found no correlation between ITPA expression and Hb decline, even after stratifying by missense variant genotypes, although examination of ITPA expression in erythrocytes or Western blot analysis of protein expression would provide additional corroborating evidence. Moreover, none of the SNPs that we genotyped in this locus was significantly associated with ITPA expression.

On the other hand, our resequencing and fine-mapping study revealed that several SNPs were in strong LD with the missense variant and were significantly associated with ribavirin-induced anemia, with *P* values varying by <1 order of magnitude. Thus, further studies are needed to identify the causal variant(s) and elucidate its functional mechanism.

Multivariate analysis demonstrated that age, baseline Hb, and rs1127354 were independently associated with severe anemia (Hb <10 g/dL) (Table 3). This finding

Table 4. Predictive Factors for Treatment Outcomes in Hepatitis C Virus Patients Treated With Peginterferon Plus Ribavirin

Variable	*P* (univariate)	*P* (multivariate)	OR	95% CI
rs1127354 (C/A)[a]	.032	.1[b]	1.4[c]	0.93–2.09
rs8099917 (T/G)[a]	4.2×10^{-10}	4.6×10^{-11}[b]	0.23[c]	0.15–0.36
Age	.000041	.004	0.97[d]	0.95–0.99
Sex	.018	.03	1.54[e]	1.04–2.27
Body mass index	.0026	.034	0.91[f]	0.86–0.98
Baseline platelet count	.000066	.017	1.05[g]	1.01–1.09
Baseline Hb level (*g/dL*)	.013	—		
Viral load (log *IU/mL*)	.00043	.00012	0.56[h]	0.42–0.75
Fibrosis (F0-2 vs F3-4)	.063	.052	0.63[i]	0.39–1.01

CI, confidence interval; Hb, hemoglobin; OR, odds ratio.
[a]Major/minor allele.
[b]Additive model.
[c]The per-minor allele OR for sustained viral response (rs1127354 AA or CA genotypes relative to CC; rs8099917 TG or GG genotypes relative to TT).
[d]Per year increase.
[e]For male patients relative to female.
[f]Per unit increase in body mass index.
[g]Per 10^4 platelet count increase.
[h]Per log viral load increase.
[i]Relative to patients with mild fibrosis (F0–F2).

suggests that rs1127354 would be a useful marker for prediction of ribavirin-induced anemia. Moreover, genetic testing of ITPA variants might be applied to establish personalized dosages in PEG-IFN and ribavirin combined therapy.

A separate multivariate analysis revealed that rs1127354 was not significantly associated with treatment outcomes, although the association was marginally significant under univariate analysis (Table 4). This might reflect decreased treatment efficacy due to dose reduction of ribavirin in patients showing severe anemia. In contrast, Fellay et al did not detect even marginal statistical significance in a similar analysis.[8] The reason for this discrepancy is unclear but may reflect a slightly higher frequency of the minor (A) (hemolysis protective) allele in the Japanese population. A similar discrepancy in the association of the ITPA variant with thiopurine intolerance between Japanese and white race has been reported.[17–19] We also found that male patients were marginally significantly more likely to respond to treatment than female patients, which may reflect the relatively high treatment age and poor response among older female patients in Japan.[20]

ITPA hydrolyses inosine triphosphate to inosine monophosphate. Several allelic variants have been described that were associated with decreased activity.[21–23] ITPA deficiency is characterized by strong accumulation of inosine triphosphate in erythrocytes.[24] A possible relationship between ITPase deficiency and adverse drug reactions to, eg, purine analogues, are documented,[19,25] although no pathological phenotypes have been found in those individuals.

Although further molecular genetic studies in relation to ribavirin-induced anemia are needed, modulation of ITPA activity might be effective to prevent severe anemia. Moreover, anti-HCV therapy in combination with an ITPA antagonist might contribute to increase sustained viral response rates by improving compliance to the therapy. On the other hand, intolerance to several therapeutic agents has been reported in patients with decreased ITPase activity.[19,25] Therefore, such combination programs should proceed but with special attention to concomitant drug administration to avoid adverse side effects.

In conclusion, we have shown that 4 polymorphisms located around the ITPA gene, including the recently reported missense variant, are strongly associated with HCV treatment-induced anemia in Japanese HCV patients. The intronic SNP, reported to affect splicing, is monoallelic in the Japanese population. Hb decline did not correlate with ITPA expression level, suggesting that the nonsynonymous SNP rs1127354 is a single causal variant associated with ribavirin-induced anemia in Japanese HCV patients. The ITPA variant can be considered to be a predictive factor for ribavirin-induced anemia in Japanese HCV patients.

Supplementary Material

Note: To access the supplementary material accompanying this article, visit the online version of *Gastroenterology* at www.gastrojournal.org, and at doi: 10.1053/j.gastro.2010.06.071.

References

1. Barrera JM, Bruguera M, Ercilla MG, et al. Persistent hepatitis C viremia after acute self-limiting posttransfusion hepatitis C. Hepatology 1995;21:639–644.
2. Hadziyannis SJ, Sette H Jr, Morgan TR, et al. Peginterferon-alpha2a and ribavirin combination therapy in chronic hepatitis C: a randomized study of treatment duration and ribavirin dose. Ann Intern Med 2004;140:346–355.
3. Manns MP, McHutchinson JG, Gordon SC, et al. Peginterferon alfa-2b plus ribavirin for initial treatment of chronic hepatitis C: a randomized trial. Lancet 2001;358:958–965.
4. Nomura H, Tanimoto H, Kajiwara E, et al. Factors contributing to ribavirin-induced anemia. J Gastroenterol Hepatol 2004;19:1312–1317.
5. Takaki S, Tsubota A, Hosaka T, et al. Factors contributing to ribavirin dose reduction due to anemia during interferon alfa2b and ribavirin combination therapy for chronic hepatitis C. J Gastroenterol 2004;39:668–673.
6. Van Vlierberghe H, Delanghe JR, De Vos M, et al. Factors influencing ribavirin-induced hemolysis. J Hepatol 2001;34:911–916.
7. Lindahl K, Schvarcz R, Bruchfeld A, et al. Evidence that plasma concentration rather than dose per kilogram body weight predicts ribavirin-induced anaemia. J Viral Hepat 2004;11:84–87.
8. Fellay J, Thompson AJ, Ge D, et al. ITPA gene variants protect against anaemia in patients treated for chronic hepatitis C. Nature 2010;464:405–408.
9. Ohnishi Y, Tanaka T, Ozaki K, et al. A high-throughput SNP typing system for genome-wide association studies. J Hum Genet 2001;46:471–477.
10. Suzuki A, Yamada R, Chang X, et al. Functional haplotypes of PADI4, encoding citrullinating enzyme peptidylarginine deiminase 4, are associated with rheumatoid arthritis. Nat Genet 2003;34:395–402.
11. Gabriel SB, Schaffner SF, Nguyen H, et al. The structure of haplotype blocks in the human genome. Science 2002;296:2225–2229.
12. Desmet VJ, Gerber M, Hoofnagle JH, et al. Classification of chronic hepatitis: grading and staging. Hepatology 1994;19:1513–1520.
13. Ge D, Fellay J, Thompson AJ, et al. Genetic variation in IL28B predicts hepatitis C treatment-induced viral clearance. Nature 2009;461:399–401.
14. Tanaka Y, Nishida N, Sugiyama M, et al. Genome-wide association of IL28B with response to pegylated interferon-alpha and ribavirin therapy for chronic hepatitis C. Nat Genet 2009;41:1105–1109.
15. De Franceschi L, Fattovich G, Turrini F, et al. Hemolytic anemia induced by ribavirin therapy in patients with chronic hepatitis C virus infection: role of membrane oxidative damage. Hepatology 2000;31:997–1004.
16. Fried MW, Shiffman ML, Reddy R, et al. Peginterferon alfa-2a plus ribavirin for chronic hepatitis C virus infection. N Engl J Med 2002;347:975–982.
17. van Dieren JM, van Vuuren AJ, Kusters JG, et al. ITPA genotyping is not predictive for development of side effects in AZA treated inflammatory bowel disease patients. Gut 2005;54:1664.

18. Gearry RB, Roberts RL, Barclay ML, et al. Lack of association between the ITPA 94C>A polymorphism and adverse effects from azathioprine. Pharmacogenetics 2004;14:779–781.
19. Uchiyama K, Nakamura M, Kubota T, et al. Thiopurine S-methyltransferase and inosine triphosphate pyrophosphohydrolase genes in Japanese patients with inflammatory bowel disease in whom adverse drug reactions were induced by azathioprine/6-mercaptopurine treatment. J Gastroenterol 2009;44:197–203.
20. Sezaki H, Suzuki F, Kawamura Y, et al. Poor response to pegylated interferon and ribavirin in older women infected with hepatitis C virus of genotype 1b in high viral loads. Dig Dis Sci 2009;54:1317–1324.
21. Sumi S, Marinaki AM, Arenas M, et al. Genetic basis of inosine triphosphate pyrophosphohydrolase deficiency. Hum Genet 2002; 111:360–367.
22. Cao H, Hegele RA. DNA polymorphisms in ITPA including basis of inosine triphosphatase deficiency. J Hum Genet 2002;47:620–622.
23. Arenas M, Duley J, Sumi S, et al. The ITPA c.94C>A and g.IVS2+21A>C sequence variants contribute to missplicing of the ITPA gene. Biochim Biophys Acta 2007;1772:96–102.
24. Vanderheiden BS. Genetic studies of human erythrocyte inosine triphosphatase. Biochem Genet 1969;3:289–297.
25. von Ahsen N, Armstrong VW, Behrens C, et al. Association of inosine triphosphatase 94CNA and thiopurine-methyltransferase deficiency with adverse events and study drop-outs under azathioprine therapy in a prospective Crohn disease study. Clin Chem 2005;51:2282–2288.

Received April 24, 2010. Accepted June 30, 2010.

Reprint requests

Address requests for reprints to: Kazuaki Chayama, MD, PhD, Department of Medical and Molecular Science, Division of Frontier Medical Science, Programs for Biomedical Research Graduate School of Biomedical Science, Hiroshima University, 1-2-3 Kasumi, Minami-ku, Hiroshima 734-8551, Japan. e-mail: chayama@hiroshima-u.ac.jp; fax: (81) 82-255-6220.

Acknowledgments

The authors thank the patients who agreed to participate in this study. We also thank the team members at Toranomon Hospital, Hiroshima University Hospital, and Hiroshima Liver Study Group for clinical sample collection. We thank T. Yokogi, H. Ishino, and K. Izumoto, T. Takajyo, and J. Sakamiya for technical assistance; and other members of the RIKEN Center for Genomic Medicine and Hiroshima University for assistance with various aspects of this study.

Conflicts of interest

The authors disclose no conflicts.

Funding

This study was supported in part by RIKEN and by Dainippon Sumitomo Pharma Co, Ltd.

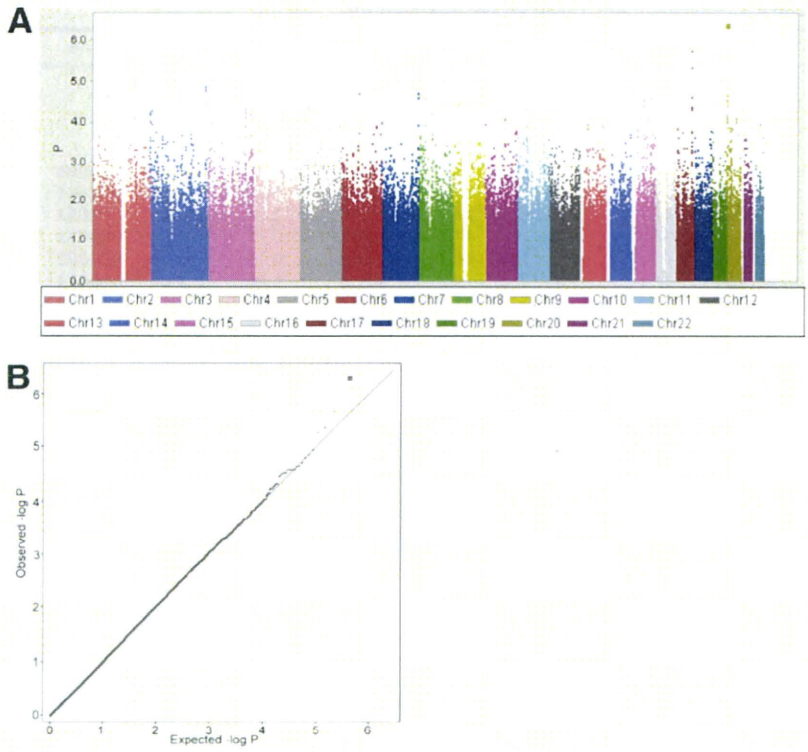

Supplementary Figure 1. Results of the genome-wide association study-1 (GWAS-1). (*A*) log10 *P* value plot at the first stage. Each *P* value was calculated by linear regression. The *large dot* corresponds to the single nucleotide polymorphism (SNP) with the strongest association, located in the DDRGK1 gene. (*B*) Quantile-quantile plot for GWAS-1. *Dots* represent *P* values of each SNP that passed the quality control filters. Only one SNP (*large dot*) in the DDRGK1 gene attained genome-wide significance after GWAS-2. The inflation factor λ was estimated to be 1.004.

Supplementary Table 1. Results of Resequencing and Fine-Mapping

SNP ID	Chr20	Allele 1	Allele 2	MAF%[a]	P(HWE)[b]	D'[c]	R^{2c}	Gene	Location	Function
—	3117545	—	T	37.2	0.3	1.00	0.11			
rs71724704	3117729	A	G	26.6	0.082	0.37	0.07			
rs71724706	3118172	C	T	24.4	0.173	0.36	0.07			
—	3118992	—	AG	21.7	0.880	1.00	0.05			
rs2295546	3119628	G	A	37.0	0.417	1.00	0.11	DDRGK1	intron9	
rs2295547	3120246	A	C	39.1	0.979	1.00	0.12	DDRGK1	intron7	
rs6051628	3120679	T	C	13.3	0.796	1.00	0.03	DDRGK1	intron6	
rs11472024	3120771	AT	—	47.7	0.555	0.77	0.11	DDRGK1	intron6	
rs6051629	3121589	C	T	46.7	0.573	0.79	0.13	DDRGK1	intron6	
rs76284374	3121710	G	A	8.7	0.518	0.66	0.23	DDRGK1	intron6	
rs8119219	3121907	T	C	37.8	0.789	1.00	0.12	DDRGK1	intron6	
rs6515773	3122105	C	T	38.0	0.681	1.00	0.12	DDRGK1	intron6	
rs7274047	3122268	C	T	38.0	0.681	1.00	0.12	DDRGK1	intron6	
rs2295548	3123260	C	T	37.8	0.789	1.00	0.12	DDRGK1	intron6	
rs2295549	3123556	G	C	46.7	0.573	0.79	0.13	DDRGK1	intron5	
rs2295550	3123694	G	A	37.8	0.789	1.00	0.12	DDRGK1	intron5	
rs2295551	3123742	A	G	37.8	0.789	1.00	0.12	DDRGK1	intron5	
rs2295552	3124009	T	C	38.9	0.903	1.00	0.13	DDRGK1	intron4	
rs7263489	3124072	C	T	32.6	0.550	1.00	0.09	DDRGK1	intron4	
rs4815575	3124443	T	A	34.4	0.663	1.00	0.11	DDRGK1	intron4	
rs6051633	3125184	A	G	35.9	0.488	0.06	0.00	DDRGK1	intron4	
rs6051634	3125188	A	G	31.5	0.329	0.18	0.00	DDRGK1	intron4	
rs6037495	3125195	C	T	29.3	0.147	0.01	0.00	DDRGK1	intron4	
rs34868732	3126817	G	A	15.2	0.941	1.00	0.03	DDRGK1	intron4	
rs6051636	3126949	C	A	47.8	0.143	0.80	0.13	DDRGK1	intron4	
rs67154167	3127366	C	A	19.6	0.246	1.00	0.05	DDRGK1	intron4	
rs6051638	3127897	T	C	46.7	0.248	0.81	0.13	DDRGK1	intron4	
rs8121983	3128226	T	C	23.9	0.0004	1.00	0.06	DDRGK1	intron4	
rs6051639	3128283	A	C	46.7	0.003	0.78	0.10	DDRGK1	intron4	
rs41281852	3128973	C	T	21.3	0.001	1.00	0.06	DDRGK1	intron3	
rs6051640	3130893	C	T	16.0	0.831	1.00	0.92	DDRGK1	intron2	
rs2326083	3131348	G	A	35.9	0.488	1.00	0.10	DDRGK1	intron2	
rs4630837	3131364	C	T	15.2	0.223	1.00	1.00	DDRGK1	intron2	
rs731282	3131404	C	T	19.6	0.823	1.00	0.05	DDRGK1	intron2	
rs2295553	3132134	T	C	46.7	0.573	1.00	0.21	DDRGK1	intron1	
rs11697186	3133123	A	T	15.2	0.223	1.00	1.00	DDRGK1	intron1	
rs6037498	3133982	C	T	16.3	0.186	1.00	0.92			
—	3134718	G	A	15.6	0.217	1.00	1.00			
rs66696167	3135609	G	A	30.7	0.543	1.00	0.08			
rs6139030	3135733	T	C	15.9	0.210	1.00	0.92			
—	3136021	T	C	4.8	0.0003	0.51	0.05			
rs6076491	3136521	G	A	17.4	0.166	1.00	0.84			
—	3136833	—	T	28.6	0.0001	0.25	0.01			
rs6051644	3137043	T	C	29.3	0.092	0.15	0.00			
rs57534080	3137091	C	T	33.7	0.150	1.00	0.09			
rs6037500	3137117	A	G	16.3	0.202	1.00	0.92			
rs6139031	3137982	G	A	16.7	0.180	1.00	0.92			
rs45620433	3138039	C	G	34.4	0.663	1.00	0.10			
rs6115814	3138790	G	T	20.0	0.852	1.00	0.05	ITPA	intron1	
rs6051646	3139068	G	A	15.6	0.217	0.73	0.54	ITPA	intron1	
rs6037501	3139205	G	T	34.1	0.552	1.00	0.09	ITPA	intron1	
rs2422860	3139464	A	G	28.4	0.739	1.00	0.08	ITPA	intron1	
rs73076878	3139725	GAA	—	50.0	1.000	1.00	0.19	ITPA	intron1	
rs59835378	3140881	A	G	30.7	0.920	1.00	0.08	ITPA	intron1	
rs6084304	3141486	C	T	48.9	0.760	1.00	0.18	ITPA	intron1	
rs6084305	3141508	T	A	47.7	0.537	0.68	0.10	ITPA	intron1	
rs11087570	3141732	G	A	17.0	0.173	1.00	0.04	ITPA	intron1	
rs1127354	3141842	C	A	15.9	0.210	—	—	ITPA	exon2	P32T
rs8362	3141978	A	G	29.5	0.401	0.24	0.00	ITPA	exon3	Q46Q
rs67002563	3142173	G	A	15.6	0.217	1.00	1.00	ITPA	intron3	
rs35991941	3142237	A	G	33.3	1.000	1.00	0.09	ITPA	intron3	
rs76430681	3142997	C	A	5.7	0.689	1.00	0.32	ITPA	intron3	
rs6076494	3143627	G	A	27.9	0.622	1.00	0.08	ITPA	intron4	

Supplementary Table 1. Continued

SNP ID	Chr20	Allele 1	Allele 2	MAF%[a]	P(HWE)[b]	D'[c]	R^2[c]	Gene	Location	Function
rs11087571	3144253	A	G	48.9	0.464	1.00	0.18	ITPA	intron5	
rs73573878	3145192	C	T	17.4	0.532	1.00	0.04	ITPA	intron5	
rs6139032	3145512	T	C	48.9	0.553	0.72	0.11	ITPA	intron5	
rs6051650	3146442	A	T	50.0	0.662	1.00	0.19	ITPA	intron5	
—	3146575	C	T	31.5	0.079	0.13	0.01	ITPA	intron5	
rs4815576	3147446	C	G	43.5	0.309	0.61	0.06	ITPA	intron6	
rs6107257	3148825	C	T	27.4	0.509	0.12	0.01	ITPA	intron6	
rs4813632	3149739	T	C	26.1	0.996	0.26	0.00	ITPA	intron6	
rs6139034	3150069	T	C	29.5	0.935	1.00	0.07	ITPA	intron6	
rs6139035	3150129	C	T	30.4	0.898	1.00	0.09	ITPA	intron6	
rs6139036	3150189	C	T	43.5	0.768	0.52	0.04	ITPA	intron6	
rs10537787	3150225	—	TGGT	29.3	0.978	1.00	0.08	ITPA	intron6	
rs6107258	3150636	G	A	19.6	0.823	1.00	0.05	ITPA	intron7	
rs66724923	3150764	A	T	48.9	0.553	1.00	0.19	ITPA	intron7	
rs2236206	3151950	A	T	30.9	0.719	1.00	0.08	ITPA	intron7	
rs9101	3152084	A	G	40.2	0.377	1.00	0.13	ITPA	exon8	E187E
rs13830	3152231	G	A	14.9	0.230	1.00	1.00	ITPA	exon8	3'UTR
rs4297961	3153008	C	T	25.0	0.024	0.00	0.00			
rs73891130	3153161	C	T	19.1	0.794	1.00	0.05			
rs6051655	3154068	G	A	19.6	0.823	1.00	0.05			

[a]Minor allele frequency.
[b]Hardy–Weinberg *P* value.
[c]The correlation coefficient with the missense single nucleotide polymorphism in the inosine triphosphate pyrophosphatase gene (rs1127354).

Journal of General Virology (2010), **91**, 1854–1864 DOI 10.1099/vir.0.019224-0

HBx protein is indispensable for development of viraemia in human hepatocyte chimeric mice

Masataka Tsuge,[1,2,3] Nobuhiko Hiraga,[1,3] Rie Akiyama,[1,3] Sachi Tanaka,[1,3] Miyuki Matsushita,[1,3] Fukiko Mitsui,[1,3] Hiromi Abe,[1,4] Shosuke Kitamura,[1,3] Tsuyoshi Hatakeyama,[1,3] Takashi Kimura,[1,3] Daiki Miki,[1,3] Nami Mori,[1,3] Michio Imamura,[1,3] Shoichi Takahashi,[1,3] C. Nelson Hayes[1,3] and Kazuaki Chayama[1,3,4]

Correspondence
Kazuaki Chayama
chayama@hiroshima-u.ac.jp

[1]Department of Medicine and Molecular Science, Division of Frontier Medical Science, Programs for Biomedical Research, Graduate School of Biomedical Sciences, Hiroshima University, Hiroshima, Japan

[2]Natural Science Center for Basic Research and Development, Hiroshima University, Hiroshima, Japan

[3]Liver Research Project Center, Hiroshima University, Hiroshima, Japan

[4]Laboratory for Liver Diseases, SNP Research Center, The Institute of Physical and Chemical Research (RIKEN), Yokohama, Japan

The non-structural X protein, HBx, of hepatitis B virus (HBV) is assumed to play an important role in HBV replication. Woodchuck hepatitis virus X protein is indispensable for virus replication, but the duck hepatitis B virus X protein is not. In this study, we investigated whether the HBx protein is indispensable for HBV replication *in vivo* using human hepatocyte chimeric mice. HBx-deficient (HBx-def) HBV was generated in HepG2 cells by transfection with an overlength HBV genome. Human hepatocyte chimeric mice were infected with HBx-def HBV with or without hepatic HBx expression by hydrodynamic injection of HBx expression plasmids. Serum virus levels and HBV sequences were determined with mice sera. The generated HBx-def HBV peaked in the sucrose density gradient at points equivalent to the generated HBV wild type and the virus in a patient's serum. HBx-def HBV-injected mice developed measurable viraemia only in continuously HBx-expressed liver. HBV DNA in the mouse serum increased up to 9 $\log_{10}$ copies ml^{-1} and the viraemia persisted for more than 2 months. Strikingly, all revertant viruses had nucleotide substitutions that enabled the virus to produce the HBx protein. It was concluded that the HBx protein is indispensable for HBV replication and could be a target for antiviral therapy.

Received 15 December 2009
Accepted 5 March 2010

INTRODUCTION

Chronic hepatitis B virus (HBV) infection is associated with the development of virus-related liver diseases, including chronic hepatitis, liver cirrhosis and hepatocellular carcinoma (HCC). HBV is a member of the family *Hepadnaviridae*, which consists of hepatotropic, small DNA viruses that infect their respective animal hosts (Ando *et al.*, 1999; Ganem & Schneider, 2001; Raney & McLachlan, 1991). HBV particles contain a 3.2 kb partially double-stranded circular DNA genome encoding four open reading frames (ORFs). The preS/S, pre-core/core, polymerase/reverse transcriptase and non-structural X protein (HBx) mRNAs are transcribed from each of the four ORFs (Seeger & Mason, 2000; Tang *et al.*, 2001). Although previous works have demonstrated that HBx protein is necessary for maximal HBV replication in cultured cells (Bouchard *et al.*, 2001; Keasler *et al.*, 2007; Leupin *et al.*, 2005; Tang *et al.*, 2005) and in mouse hepatocytes (Keasler *et al.*, 2007), the precise function of HBx in the virus life cycle remains poorly defined in human hepatocytes under physiological conditions because there is no natural infection–replication system available. Accordingly, all previous work has been done using hepatocarcinoma cell lines with transfection or mouse hepatocytes with hydrodynamic injection. Analysis of HBx under physiological conditions will provide more accurate information for the function of the HBx protein.

The nucleotide and amino acid sequences of the X genes are well-conserved among all mammalian hepadnaviruses. Expression of HBx protein in hepatocytes has been reported

The GenBank/EMBL/DDBJ accession number for the nucleotide sequence of the HBV genome cloned into plasmid pTRE-HB-wt is AB206817.

both in humans (Su *et al.*, 1998) and in woodchucks (Dandri *et al.*, 1996; Jacob *et al.*, 1997). Previous reports have shown that the X protein of the woodchuck hepatitis virus (WHV) is important for the virus life cycle (Chen *et al.*, 1993; Sitterlin *et al.*, 2000a; Zhang *et al.*, 2001; Zoulim *et al.*, 1994). In contrast, in non-oncogenic avian hepatitis viruses, such as duck hepatitis B virus (DHBV), the X protein (DHBx) is not necessary for virus replication *in vivo* (Meier *et al.*, 2003). The HBx and WHV X proteins (WHx) localize both in the cytoplasm and in the nucleus (Dandri *et al.*, 1998; Doria *et al.*, 1995; Sitterlin *et al.*, 2000b; Wang *et al.*, 1991), and both of them have similar multi-phasic activities for transcription, DNA repair, cell growth and apoptotic cell death in tissue-culture cells (Arbuthnot *et al.*, 2000; Murakami, 2001). HBx and WHx have also been shown to stimulate virus replication in cell lines by activating viral transcription (Colgrove *et al.*, 1989; Melegari *et al.*, 2005; Zhang *et al.*, 2001) or by enhancing the reverse transcription activity of the viral polymerase (Bouchard *et al.*, 2001; Klein *et al.*, 1999). Although it has been shown that the WHx protein is indispensable for virus replication *in vivo* (Zoulim *et al.*, 1994), which of the above functions is indispensable remains unknown. As HBV infects only humans and chimpanzees, it has been difficult to perform intensive studies *in vivo*.

Recently, Mercer *et al.* (2001) reported that transplanted human hepatocytes in SCID mice homozygous for the Alb-uPA transgene resulted in replacement of the mouse liver. They also reported that the highly replaced mice are susceptible to hepatitis C virus (Mercer *et al.*, 2001). Tateno *et al.* (2004) also created human hepatocyte chimeric mice with an improved replacement rate. Using this chimeric mouse model and the cell-culture-created HBV, we showed previously that hepatitis B e antigen (HBeAg) is dispensable for virus infection and replication (Tsuge *et al.*, 2005).

In this study, we tested whether the cell-culture-generated HBx-defective (HBx-def) HBV infects and replicates in the chimeric mice. As HBx-def HBV did not develop measurable viraemia, we expressed the HBx protein in the chimeric mouse liver by hydrodynamically injecting HBx-expression plasmid. It was noted that this *trans*-complementation of HBx helped the replication of HBx-def virus in the chimeric mice, and revertant viruses showed nucleotide substitutions that reversed the introduced stop codon [CAA to TAA created by a C-to-T point mutation at nt 1395 (aa 7) in the HBx gene; Fig. 1a] and restored expression. The HBx protein is thus indispensable for infection and proliferation of HBV. The protein thus might be a target for therapy development against HBV.

RESULTS

Production of HBV particles and antigens in cell culture and effect of HBx ablation

We initially examined nucleotide sequences of the cell-line-produced HBV by direct sequencing of the PCR products using cell-culture supernatants. As expected, HBV DNA was released from HepG2 cells transfected with the HBx-def plasmid with an introduced stop codon mutation by calcium phosphate precipitation (data not shown). We then analysed hepatitis B surface antigen (HBsAg), HBeAg and HBV DNA in the supernatants 3 days after transfection. While HBV DNA titres were not significantly different between the wild-type (WT)- and HBx-def HBV-transfected cultures, the HBsAg and the HBeAg levels were significantly lower in HBx-def HBV- than in WT-transfected cultures (Fig. 1b).

To examine the particle formation in the transfection experiments, we analysed the density of generated HBV by sucrose density gradient sedimentation analysis. The density of the cell-culture-produced HBx-def HBV was compared with those of WT HBV and HBV obtained from human serum. As shown in Fig. 1(c), each of the three preparations of HBV sedimented at sucrose density 1.18 g ml^{-1}, suggesting that cell-culture-produced HBV particles were similar to those obtained from human serum.

Infectivity of HBx-def HBV particles

To analyse the infectivity of HBx-def HBV, we inoculated cell-culture-produced recombinant HBV (WT HBV or HBx-def HBV) into chimeric mice. All seven mice injected with cell-culture-generated WT HBV developed measurable viraemia 2–7 weeks after inoculation. The virus titre reached 6–10 log_{10} copies ml^{-1} and the viraemia persisted for more than 4 months (Fig. 2a). In contrast, we did not observe any measurable viraemia in HBx-def HBV-injected mice within a period of 16 weeks after inoculation (Fig. 2b). Only five of 16 HBx-def HBV-inoculated mice became occasionally positive for HBV DNA by nested PCR assay. We then examined the mouse livers 14 weeks after inoculation by immunohistochemical staining with anti-HB core (HBc) antibody. As shown in Fig. 2(c), human hepatocytes of WT-injected mice were positive for HBV core antigen (HBcAg). In contrast, the staining was negative in mouse liver injected with HBx-def HBV.

Effect of *trans*-complementation of entire and partial HBx protein on replication of HBx-def HBV

We then investigated the effect of *trans*-complementation of the HBx protein both *in vitro* and *in vivo*. Since the C-terminal two-thirds (aa 51–154) domain of HBx has been reported to contain a transactivation domain (Tang *et al.*, 2005), we constructed three plasmids (full length and residues 1–50 and 51–154), as shown in Fig. 3(a). To analyse the effect of co-transfection of these three plasmids on intracellular replication of HBV, the cells transfected using *Trans*IT-LT1 reagent were harvested 24 h after transfection and analysed by Southern blotting. As shown in Fig. 3(b), *trans*-complementation of HBx enhanced the

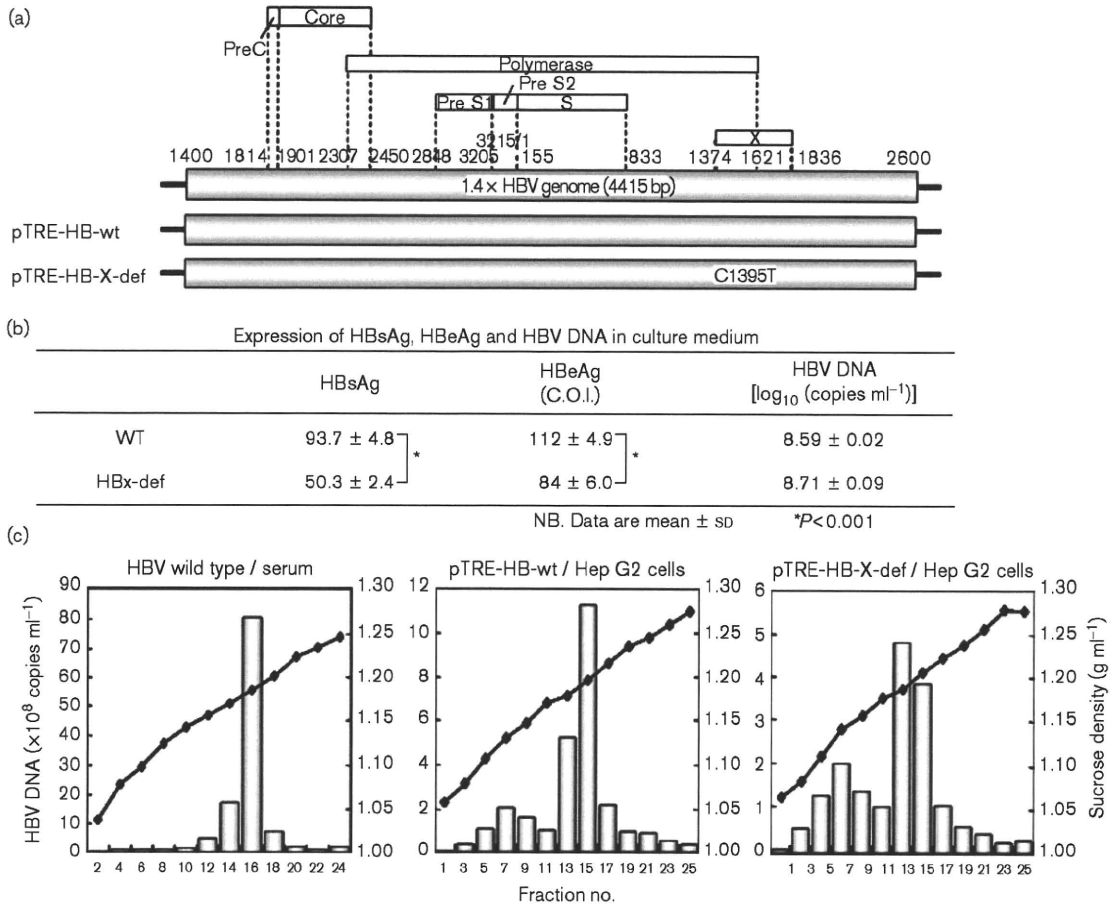

Fig. 1. Construction of HBV expression plasmids. (a) Wild type (WT) 1.4× genome length HBV was cloned into the pTRE2hyg vector (pTRE-HB-wt) and a nucleotide substitution, C1395T, was introduced to create the HBx-def mutant pTRE-HB-X-def. (b) Comparison of expression of HBsAg, HBeAg and HBV DNA in culture medium between WT and HBx-def. (c) Sucrose density gradient analysis of HBV particles (◆) and HBV DNA copies (bars) obtained from a serum sample (left) and supernatants from a cell culture transfected with WT HBV (pTRE-HB-wt, middle) and HBx-def pTRE-HB-X-def. C.O.I., cut-off index.

replication of HBV to the WT level. The effects of HBx protein were also evident on the expression of HBsAg (Fig. 3c) and HBeAg (Fig. 3d). As reported previously, the effect of the C-terminal two-thirds (aa 51–154) of the HBx protein was stronger than that of the entire protein and the N-terminal one-third (aa 1–50) (Tang *et al.*, 2005). The production of replication intermediates was increased similarly by co-transfection of the X proteins (Fig. 3e). To further study the effect of HBx expression, we analysed the levels of intracellular core protein expression. As shown in Fig. 4(a), the expression levels of the core protein were upregulated with the expression of the entire (WT) and C-terminal two-thirds (aa 51–154) of the HBx protein. Immunocytochemical analysis showed that only the cells with strong HBx protein expression were stained with the core protein (Fig. 4b). The core and HBx proteins in these cells were stained mainly in the cytoplasm.

Expression of HBx protein in mouse liver by hydrodynamic injection

Next, we expressed the HBx protein in the chimeric mouse liver with hydrodynamic injection. As shown in Fig. 5(a), a dose-dependent expression of the HBx protein with a haemagglutinin (HA) tag was confirmed by Western blot analysis. Although Henkler *et al.* (2001) showed an aggregation of HBx under the control of the human cytomegalovirus (CMV) promoter, we were able to observe expression of properly sized HBx. Immunohistochemical analysis also revealed HBx protein expression in the mouse

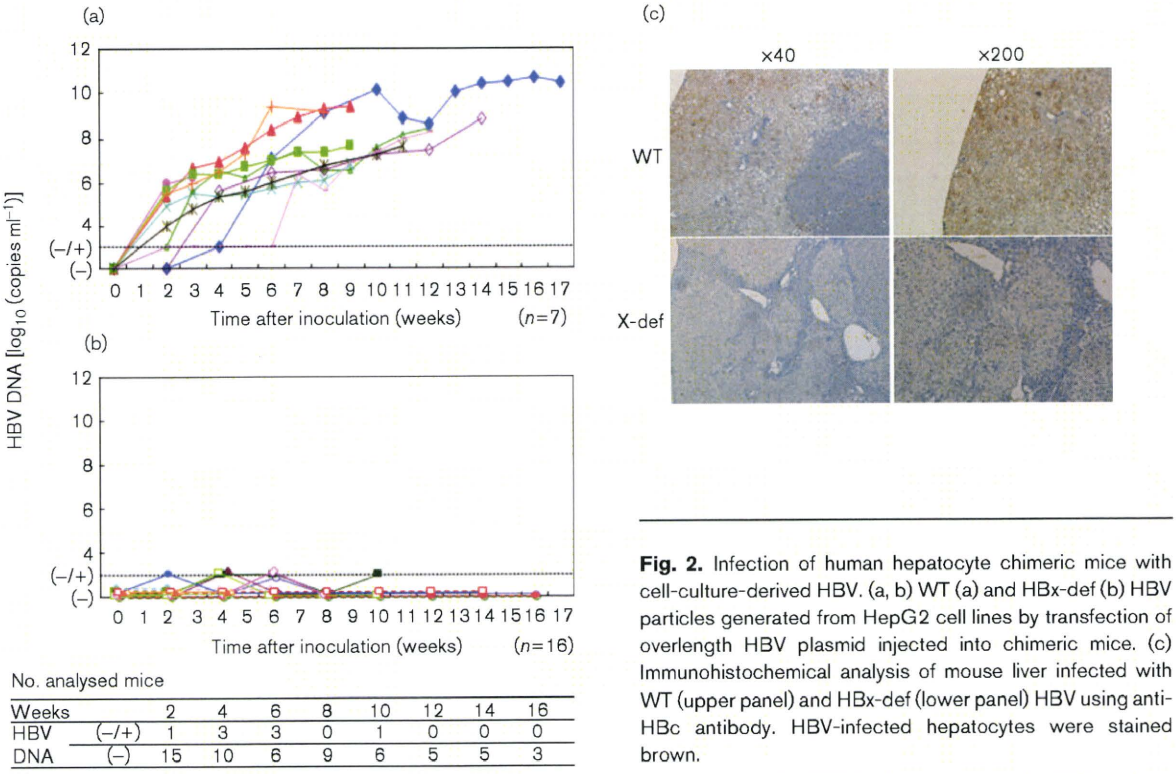

No. analysed mice

Weeks		2	4	6	8	10	12	14	16
HBV	(−/+)	1	3	3	0	1	0	0	0
DNA	(−)	15	10	6	9	6	5	5	3

Fig. 2. Infection of human hepatocyte chimeric mice with cell-culture-derived HBV. (a, b) WT (a) and HBx-def (b) HBV particles generated from HepG2 cell lines by transfection of overlength HBV plasmid injected into chimeric mice. (c) Immunohistochemical analysis of mouse liver infected with WT (upper panel) and HBx-def (lower panel) HBV using anti-HBc antibody. HBV-infected hepatocytes were stained brown.

liver. Notably, the HBx protein staining was strong around the central vein (Fig. 5b).

Infection of HBx-def HBV particles with intrahepatic expression of the HBx protein

As the infection experiments with HBx-def HBV failed to result in measurable viraemia (Fig. 2b), we then tried to infect HBx-def HBV after expression of HBx protein by hydrodynamic injection. As shown in Fig. 6(a), six of seven mice developed measurable viraemia 2–8 weeks after inoculation. The incidence of measurable viraemia was significantly higher in mice that received hydrodynamic injection than in those without (Fig. 2b versus Fig. 6a, $P<0.0001$). Immunohistochemical analysis of the infected mice showed simultaneous staining for human serum albumin (hAlb) and HBcAg in the same portion of the liver (Fig. 6b).

Sequence analysis of inocula and the infected mouse sera

We analysed nucleotide sequences of the virus recovered from all six infected mice and compared them with those of inoculated HBx-def HBV. As shown in Fig. 7(a), direct sequencing analyses of the amplified HBV DNA products showed that all revertant viruses had T1395C (mouse MHX#1, 3, 5–7) or T1395A (mouse MHX#2) point mutations, which reverted the introduced stop codon to amino acids. We further analysed nucleotide sequences of HBV by cloning and sequencing using serum samples obtained from two mice (MHX#1, 33 clones; MHX#2, 38 clones) (Fig. 7b). Only one of 33 clones obtained from MHX#1 and none of the 38 clones from MHX#2 had the stop codon mutation that was introduced into the transfected plasmid.

DISCUSSION

In previous studies, HBx has been reported to be a multifunctional protein affecting cell growth and proliferation and activating transcription of mRNA (Arbuthnot *et al.*, 2000; Bouchard *et al.*, 2001; Klein *et al.*, 1999; Murakami, 2001) and virus replication in HCC cell lines (Bouchard *et al.*, 2001; Keasler *et al.*, 2007; Leupin *et al.*, 2005; Tang *et al.*, 2005) and mouse hepatocytes (Keasler *et al.*, 2007; Xu *et al.*, 2002). However, these results were obtained by introduction of HBV genomes into cells using artificial methods such as transfection, gene transfer and hydrodynamic injection. Recently, we established an *in vivo* HBV infection system using human hepatocyte chimeric mice (Tsuge *et al.*, 2005). The system enabled us to perform infection experiments using HBV-containing patient sera and cell-culture medium. Using this system,

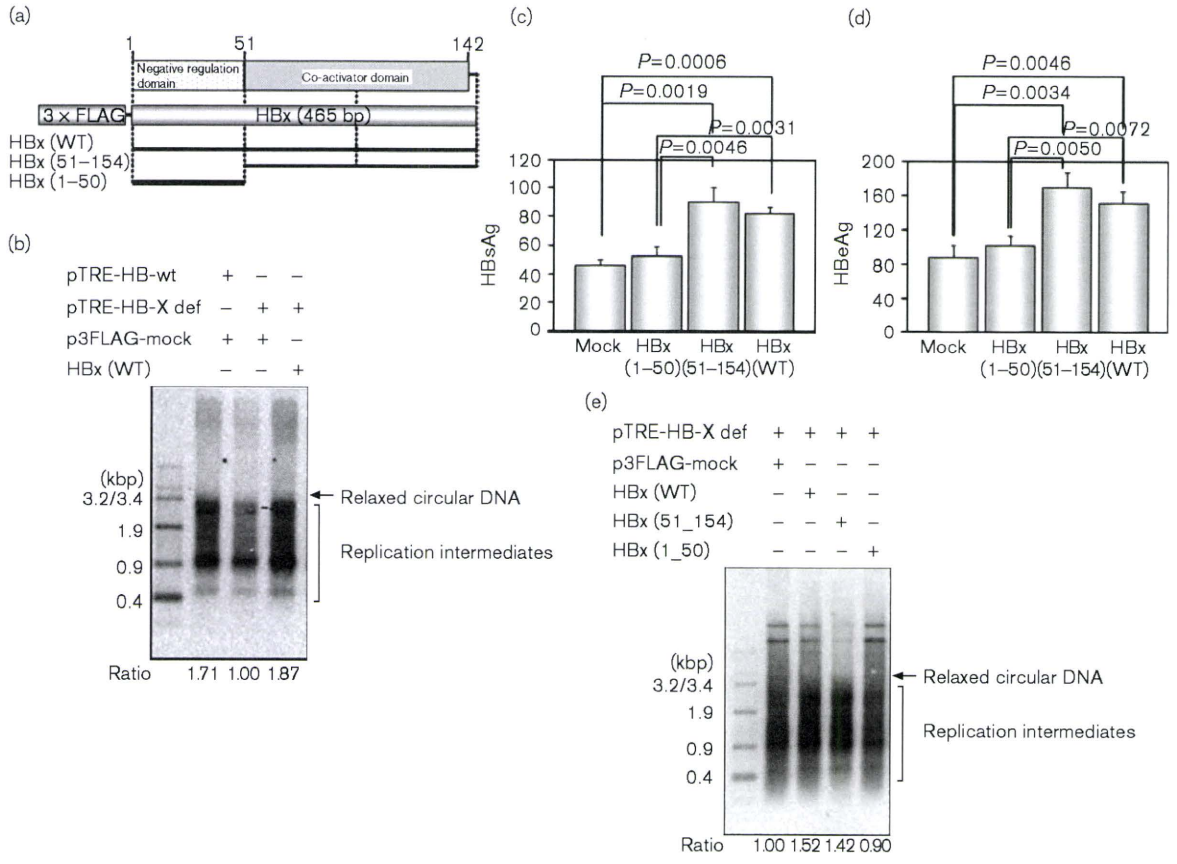

Fig. 3. Recovery of reduced formation of replication intermediate and HB antigens from HBx-def HBV by *trans*-complementation of HBx. (a) Construction of HBx expression plasmids. Full-length and deletion mutants of HBx gene were cloned into the p3FLAG-CMV10 or pcDNA3 or pcDNA3.1-3HA vector. Examples of three FLAG-tagged plasmids are shown. (b) *Trans*-complementation of HBx protein restored the reduced formation of replication intermediates of HBx-def HBV. The core-associated HBV replication intermediates were collected from HepG2 cells and detected with Southern blot hybridization with a full-length HBV probe. (c–e) Recovery of reduced production of HBsAg (c) and HBeAg (d) in culture medium and replication intermediates (e) of HBx-def HBV with *trans*-complementation of HBx expression plasmids. HBx (WT) and HBx(51–154), but not HBx(1–50), effectively enhanced the formation of HBV products. (b, e) The levels of core-associated HBV DNA are shown at the bottom of each lane. Data in (c) and (d) are mean ± SD of three experiments.

we showed previously that HBeAg is dispensable for HBV infection and active replication *in vivo* (Tsuge *et al.*, 2005). Virus replication following infection of HBV particles is quite similar to natural infection. We thus applied the system to study the function of HBx protein in this study. We also utilized hydrodynamic injection of HBx expression plasmid to *trans*-complement the defective HBx. As shown by Western blot analysis (Fig. 4a), HBx protein of the expected size was produced without development of antibody in this SCID-mouse-based model system.

This natural infection mode is quite different from previous animal studies. Virus titres of HBx-def HBV were approx. 50–99 % compared with WT HBV *in vitro* (Bouchard *et al.*, 2001; Keasler *et al.*, 2007; Leupin *et al.*, 2005; Tang *et al.*, 2005) and *in vivo* (Keasler *et al.*, 2007; Xu *et al.*, 2002). High-level HBx-def virus production seen in these experiments may be the result of expression of HBV proteins other than HBx following forced introduction of plasmids into mouse liver cells by hydrodynamic injection or transgenes. Such introduction probably resulted in virus production that is similar to *in vitro* transfection experiments using cultured cells.

In vitro experiments in this study showed that normal-density HBV particles (Fig. 1c) were produced in the absence of HBx. Curiously, the amount of HBV DNA released from the cells into the supernatant was not different between WT and HBx-def HBV, even though the

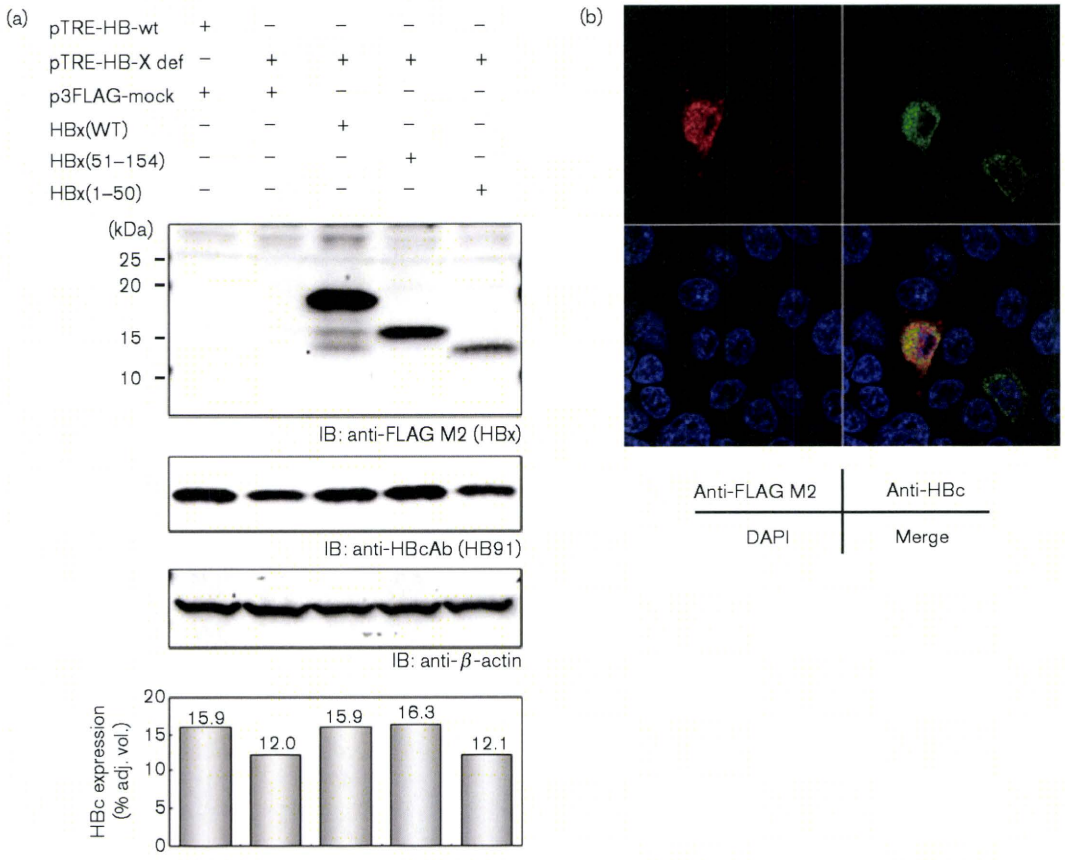

Fig. 4. Upregulation of intracellular core protein formation by *trans*-complementation of the HBx proteins. (a) Western blot analysis of intracellular proteins. Expression of the HBx proteins (percentage adjusted volume) is shown by staining the fused FLAG tag (upper panel). The membrane was also stained by the anti-HBc (middle) and anti-β-actin (lower) antibodies. Values obtained by scanning via densitometer are shown at the bottom of each lane. (b) Immunohistochemical analysis of HepG2 cells co-transfected with pTRE2-HB-X-def and p3FLAG-HBx plasmids. The expression of HBx and HBc proteins was detected by anti-FLAG (upper left) and anti-HBc (upper right) antibody, respectively. The merged image is shown in the lower right and nuclei are shown in the lower left panel. Note that only cells positive for HBx are also positive for HBc protein.

amounts of HBsAg and HBeAg as well as the amount of HBV DNA in cells were significantly greater in WT (Fig. 1b). Efficacy of release of the virus from the cells might be different between WT and HBx-def HBV. Alternatively, production of defective virus, which appeared as the second peak of HBV DNA in the sucrose gradient experiment (Fig. 1c, right panel), might be enriched in HBV DNA in the supernatant of HBx-def HBV. The reason for this discrepancy is unknown. Previous papers did not mention such production of HBV into the supernatant.

Similarly, in the absence of HBx protein *in vitro*, the formation of the replication intermediates (Fig. 3) and production of intracellular core protein (Fig. 4) continued, although their amounts were much lower. It is thus difficult to explain the inability of HBx-def HBV to infect *in vivo* simply from its transcription-activating ability, although our results confirmed that HBx has *trans*-activation ability, as reported previously (Keasler *et al.*, 2007; Tang *et al.*, 2005; Xu *et al.*, 2002). A different mode of introduction of viral nucleic acid might explain the difference seen in *in vitro* and *in vivo* experiments. In the transfection experiments, a relatively large amount of HBV DNA is introduced by transfection. In contrast, only successfully attached virus particles can introduce viral DNA into liver cells.

Strikingly, all but one (70 of 71 clones) revertant viruses had nucleotide substitutions that reversed the introduced stop codon to a coding amino acid. This is in contrast to the fact that HBV replicates in the HBx-def form in cultured cells, even though the efficacy is lower than in WT. We assumed that complemented HBx protein stimulated the replication of HBx-def HBV and increased the chance of nucleotide sequence substitutions in the HBx

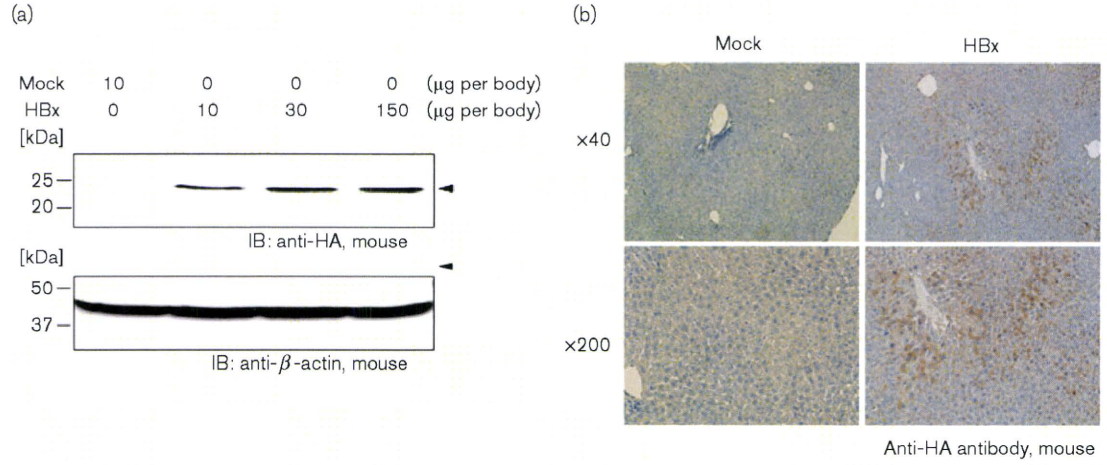

Fig. 5. Expression of HBx protein by hydrodynamic injection of HBx plasmid. (a) Liver-expressed HA-tagged HBx proteins were detected by Western blot analysis using anti-HA antibody (HA tag was used to avoid non-specific binding of anti-FLAG tag to mouse liver proteins). Dose-dependent expression of the protein was observed with different doses of the injected plasmid. (b) Immunohistochemical analysis of mouse liver using anti-HA antibody revealing expression of HBx protein. The protein was mainly expressed around the central vein.

gene, and that only revertant HBV variants predominantly increased, due to their rapid replication ability through the infection–replication cycle that only exists in the *in vivo* model. One might consider the possibility that the HBx protein works as a mutagen. However, we did not observe clear differences in the incidence of nucleotide sequence substitutions between the presence and absence of HBx (Fig. 7b and data not shown).

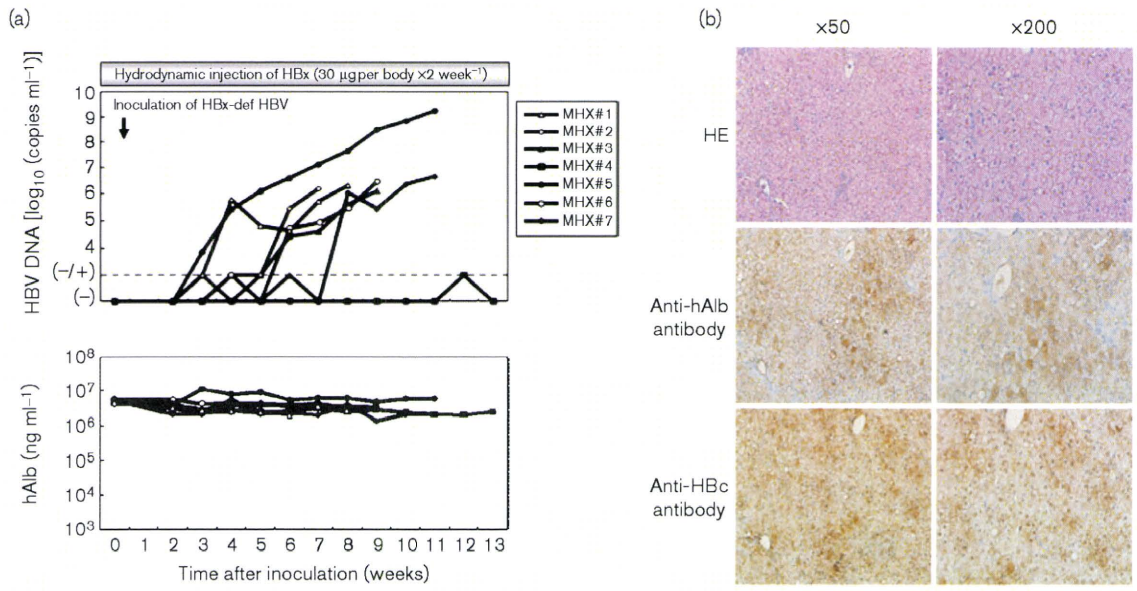

Fig. 6. Infection of HBx-def HBV particles after hydrodynamic injection of HBx expression plasmid. (a) Full-length HBx protein expression plasmid was hydrodynamically injected twice a week into human hepatocyte chimeric mice. Two weeks after the beginning of the injections, cell-culture-derived HBx-def HBV particles were injected through the tail vein. HBV DNA (upper panel) and hAlb (lower panel) were measured. (b) Immunohistochemical analysis of the infected mouse. The liver was stained with haematoxylin and eosin (HE) (upper), antibody against hAlb (middle) and anti-HBc antibody (lower).

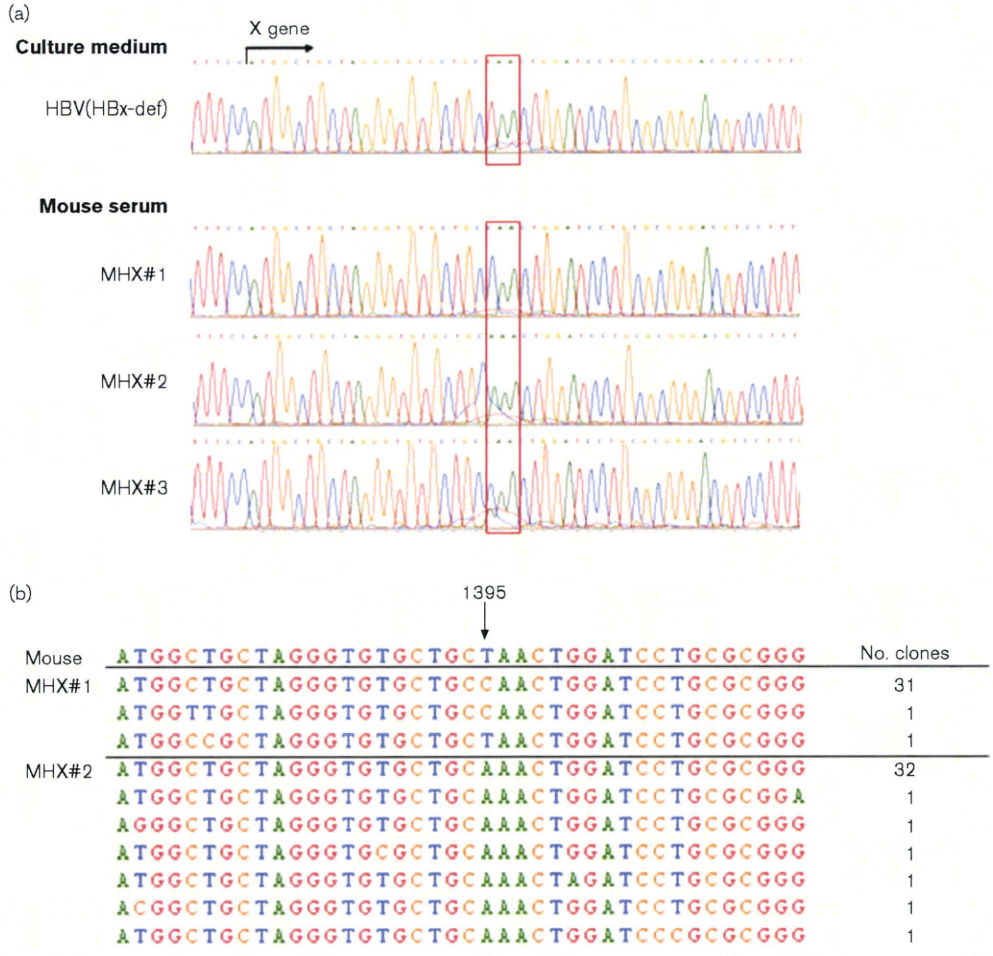

Fig. 7. Nucleotide sequence analysis of HBV recovered from HBx-def HBV-injected mice. (a) Nucleotide sequences of the HBx region of HBV determined by direct sequencing of PCR products using serum samples obtained from three mice (#1, #2 and #3 in Fig. 6a). The sequences were compared with that of inoculated HBV. Note that one of the three mice (#2) had a unique sequence different from the original sequence before introduction of the stop codon (C1395T). (b) Nucleotide sequences of the HBx gene determined by cloning and sequencing of PCR-amplified DNA from mice #1 and #2. Note that only one of 63 clones showed the introduced stop codon mutation. As we used a large amount of HBV plasmids, special care was taken to avoid contamination of DNA. Water was used as a negative control for all experiments and we observed no inappropriate amplification in these experiments.

It is thus still uncertain why the HBx protein is indispensable for virus replication *in vivo*. However, the fact that HBV cannot replicate in the absence of HBx protein may allow development of therapeutic medicine by disturbing the unknown action of HBx. To this end, it is interesting to identify a substance that binds to HBx.

The indispensability of the X protein for virus replication is a common feature shared by HBV and WHV (Chen *et al.*, 1993; Zoulim *et al.*, 1994). Both of them cause chronic infection, inflammation, fibrosis and cancer. In contrast, DHBV, which can replicate without DHBx expression, does not cause such a pathological situation (Meier *et al.*, 2003). Further analysis of the X protein may pave the way to clarify the mechanism of cancer development caused by HBV infection.

METHODS

Human hepatocyte chimeric mice experiments. Care of $uPA^{+/+}/SCID^{+/+}$ mice and transplantation of human hepatocytes were performed as described previously (Tateno *et al.*, 2004). The experiments were performed in accordance with the guidelines of the local committee for animal experiments at Hiroshima University. Infection, extraction of serum samples and sacrifice were performed under ether anaesthesia as described previously (Tateno *et al.*, 2004).

hAlb in mouse serum was measured with a Human Albumin ELISA Quantification kit (Bethyl Laboratories Inc.) according to the instructions provided by the manufacturer. Serum samples obtained from mice were aliquotted and stored in liquid nitrogen until use.

Analysis of HBV markers. HBsAg and HBeAg were measured using a commercially available ELISA kit (Abbott). For quantitative analysis of HBV DNA, 10 μl mouse serum sample or 100 μl of culture supernatant was used. DNA was extracted from these samples using the SMITEST R&D (Genome Science Laboratories) and dissolved in 20 μl H_2O, and HBV DNA was quantified by real-time PCR using the 7300 Real-Time PCR System (Applied Biosystems). Amplification was performed as described previously (Tsuge *et al.*, 2005). The lower detection limit of this assay is 300 copies. For detection of small amounts of HBV DNA, we also performed nested PCR. The amplification conditions were as described previously (Tsuge *et al.*, 2005).

Plasmid construction. The construction of wild-type (WT) HBV 1.4 genome length, pTRE-HB-wt, was described previously (Tsuge *et al.*, 2005). We used pTRE2 vector without pTet-off vector and doxycycline because a sufficient amount of HBV transcripts was produced from internal HBV promoters, and transcription from the pTRE2 promoter is negligible under these conditions. The nucleotide sequence of the HBV genome that we cloned into plasmid pTRE-HB-wt was deposited in GenBank under accession number AB206817. A modified plasmid, pTRE-HB-X-def, was generated by introducing a C-to-T point mutation at nt 1395 (aa 7) to create a stop codon (CAA to TAA) in the HBx gene (Fig. 1a). The substitution was introduced by using a QuikChange Site-Directed Mutagenesis kit (Stratagene). For the construction of the HBx gene expression plasmid, the HBx gene was amplified from pTRE-HB-wt and cloned into pcDNA3, pcDNA3-3×HA, p3×FLAG-CMV10 vectors and designated pcDNA-HBx, pcDNA3-HA-HBx, p3FLAG-HBx, respectively. Partially truncated HBx plasmids, with a deletion of the N-terminal 50 aa [HBx(51–154)] and the C-terminal 50 aa [HBx(1–50)], were also cloned into pcDNA3 or p3FLAG-CMV10 vectors.

Transfection of HepG2 cell lines with HBV expression plasmids. HepG2 cells were grown in Dulbecco's modified Eagle's medium supplemented with 10% (v/v) fetal bovine serum at 37 °C and under 5% CO_2. For functional analysis of the HBx protein *in vitro*, the HBV or HBx-def HBV expression plasmid was transfected with/without HBx expression plasmid using *Trans*IT-LT1 (Mirus) reagent according to the instructions provided by the supplier. Three to five days after transfection, core-associated HBV DNA was extracted from cells for HBV DNA quantification (Noguchi *et al.*, 2005). For analysing the infectivity of recombinant HBV particles, HBV expression plasmids were transiently transfected into HepG2 cells. The cells were seeded to semi-confluence in 90 mm dishes. WT HBV particles were generated from cells transfected with 20 μg pTRE2-HB-wt by calcium phosphate precipitation. HBx-def HBV particles were also generated from cells co-transfected with 10 μg pTRE2-HB-X-def and 10 μg pcDNA-HBx. Three days after transfection, the culture medium was collected and stored in liquid nitrogen until use.

Analysis of cell-culture-produced HBV by sucrose density gradient sedimentation. Five millilitres of HBV-positive human serum (8 $\log_{10}$ copies ml^{-1}) or 50 ml cell culture supernatant (8 $\log_{10}$ copies ml^{-1}) was layered on a 20% (w/w) sucrose cushion, and centrifuged at 24000 r.p.m. (maximum 103864 *g*) for 12 h at 4 °C with a Beckman SW28 rotor (Beckman Coulter). The precipitate was resuspended in 500 μl PBS. These HBV samples were layered on a linear 20–50% (w/w) sucrose gradient. Centrifugation was carried out at 24000 r.p.m. (maximum 102445 *g*) for 21 h at 4 °C with a Beckman SW40 rotor. The gradients were fractionated into 500 μl samples, and the density of each fraction was calculated from the weight and volume. Each fraction was diluted 10-fold and tested for HBV DNA by real-time PCR.

Analysis of replication intermediate of HBV. The cells were harvested 5 days after transfection and lysed with 250 μl lysis buffer [10 mM Tris/HCl (pH 7.4), 140 mM NaCl and 0.5% (v/v) NP-40] followed by centrifugation for 2 min at 15000 *g*. The core-associated HBV genome was immunoprecipitated by mouse anti-HBV core monoclonal antibody 2A21 (Institute of Immunology, Tokyo, Japan) and subjected to Southern blot analysis after SDS/proteinase K digestion, followed by phenol extraction and ethanol precipitation. Quantitative analysis was performed by real-time PCR with SYBR Green using the 7300 Real-Time PCR System and the amounts of the replication intermediates were compared. The HBV-specific primers used for amplification were 5′-TTTGGGCATGGACATTGAC-3′ and 5′-GGTGAACAATGTTCCGGAGAC-3′. The amplification conditions included initial denaturation at 95 °C for 10 min, followed by 45 cycles of denaturation at 95 °C for 15 s, annealing at 58 °C for 5 s and extension at 72 °C for 6 s. The lower detection limit of this assay was 300 copies.

Immunocytochemistry of HepG2 cells transfected with pTRE2-HB-X-def and p3FLAG-HBx plasmids. HepG2 cells were seeded to semi-confluence in two-well chamber plates. Each 1 μg pTRE2-HB-X-def and p3FLAG-HBx plasmids was co-transfected using *Trans*IT-LT1 reagent (Mirus) according to the instructions provided by the supplier. The cells were harvested 24 h after transfection and then washed with PBS and fixed with 4% (v/v) paraformaldehyde. After fixation, the cells were stained with mouse monoclonal antibody directed to FLAG (Sigma) or rabbit polyclonal antibody against hepatitis B core antigen (HBcAg; DAKO Diagnostika) as the primary antibody. The bound antibodies were detected with an Alexa Fluor 488-conjugated antibody against rabbit IgG or Alexa Fluor 568-conjugated antibody against mouse IgG, respectively (Molecular Probes). Nuclei were counterstained with 6-diamidino-2-phenylindole (DAPI) (Vector Laboratories).

Hydrodynamic injection of HBx expression plasmids. Hydrodynamic injection was performed as reported previously (Yang *et al.*, 2002) with slight modifications. As the human hepatocyte chimeric mice were quite small (12–15 g) and weak for the rapid injection and the stress, we reduced the amount of DNA solution and injection speed: 1 ml PBS containing 30 μg HBx expression plasmids was injected rapidly through the mouse tail vein within 30 s. For analysis of infectivity of HBx-def HBV particles, the plasmids were injected twice a week.

Western blot analysis. Mouse liver tissues or transfected HepG2 cells were cooled on ice and treated with RIPA-like buffer [50 mM Tris/HCl (pH 8.0), 0.1% SDS, 1% NP-40, 150 mM sodium chloride and 0.5% sodium deoxycholate] containing protease inhibitor cocktail (Sigma). Cell lysates were separated on SDS–polyacrylamide gels [5–20% (w/v)] (Bio-Rad) and then transferred onto nitrocellulose membranes (GE Healthcare) by electroblotting. The membranes were incubated with anti-haemagglutinin fusion epitope (anti-HA) monoclonal antibody (Roche) or with anti β-actin monoclonal antibody (Sigma) followed by incubation with horseradish peroxidase-conjugated sheep anti-mouse immunoglobulin (GE Healthcare). Proteins were visualized via the ChemiDoc XRS system (Bio-Rad). Expression of HBc protein was quantified from the densities of the immunoblot signals by Quantity One software (Bio-Rad).

Immunohistochemical analysis of mouse liver. The liver specimens of HBV-infected mice were fixed with 10% buffered paraformaldehyde and embedded in paraffin blocks for histological

examination. The liver sections were stained with haematoxylin–eosin or subjected to immunohistochemical staining using an antibody against HBcAg (DAKO Diagnostika), anti-HA antibody or HSA (Bethyl Laboratories Inc.). Endogenous peroxidase activity was blocked with 0.3 % H_2O_2 and methanol. Immunoreactive materials were visualized by using a streptavidin–biotin staining kit (Histofine SAB-PO kit; Nichirei) and diaminobenzidine.

Sequence analysis of the HBV genome. Genome-length HBV DNA was amplified by PCR as described by Günther *et al.* (1995). HBV genome-length PCR products were subjected to 1 % agarose gel electrophoresis and the 3.2 kbp band was extracted using a QiaEx II Gel Extraction kit (Qiagen). Direct sequencing, cloning and sequencing (Ohishi *et al.*, 2004) were performed in an ABI PRISM 3100-Avant Genetic Analyzer (Applied Biosystems) with a Big Dye Terminator version 3.0 Cycle Sequencing Ready Reaction kit (Applied Biosystems).

Statistical analysis. All data are expressed as mean ± SD. Differences between groups were examined for statistical significance by using Student's *t*-test. A P value <0.05 denoted the presence of a statistically significant difference.

ACKNOWLEDGEMENTS

This work was carried out at the Research Center for Molecular Medicine, Faculty of Medicine, Hiroshima University, and the Analysis Center of Life Science, Hiroshima University. The authors thank Chiemi Noguchi and Waka Ohishi for their helpful discussion, Kana Kunihiro for her excellent technical assistance, and Yoshiko Nakata and Aya Furukawa for secretarial assistance. Financial support was provided by the Ministry of Education, Sports, Culture and Technology and Ministry of Health, Labour and Welfare (Grants-in-Aid for scientific research and development).

REFERENCES

Ando, T., Sugiyama, K., Goto, K., Miyake, Y., Li, R., Kawabe, Y. & Wada, Y. (1999). Age at time of hepatitis Be antibody seroconversion in childhood chronic hepatitis B infection and mutant viral strain detection rates. *J Pediatr Gastroenterol Nutr* **29**, 583–587.

Arbuthnot, P., Capovilla, A. & Kew, M. (2000). Putative role of hepatitis B virus X protein in hepatocarcinogenesis: effects on apoptosis, DNA repair, mitogen-activated protein kinase and JAK/STAT pathways. *J Gastroenterol Hepatol* **15**, 357–368.

Bouchard, M. J., Wang, L. H. & Schneider, R. J. (2001). Calcium signaling by HBx protein in hepatitis B virus DNA replication. *Science* **294**, 2376–2378.

Chen, H. S., Kaneko, S., Girones, R., Anderson, R. W., Hornbuckle, W. E., Tennant, B. C., Cote, P. J., Gerin, J. L., Purcell, R. H. & Miller, R. H. (1993). The woodchuck hepatitis virus X gene is important for establishment of virus infection in woodchucks. *J Virol* **67**, 1218–1226.

Colgrove, R., Simon, G. & Ganem, D. (1989). Transcriptional activation of homologous and heterologous genes by the hepatitis B virus X gene product in cells permissive for viral replication. *J Virol* **63**, 4019–4026.

Dandri, M., Schirmacher, P. & Rogler, C. E. (1996). Woodchuck hepatitis virus X protein is present in chronically infected woodchuck liver and woodchuck hepatocellular carcinomas which are permissive for viral replication. *J Virol* **70**, 5246–5254.

Dandri, M., Petersen, J., Stockert, R. J., Harris, T. M. & Rogler, C. E. (1998). Metabolic labeling of woodchuck hepatitis B virus X protein in naturally infected hepatocytes reveals a bimodal half-life and association with the nuclear framework. *J Virol* **72**, 9359–9364.

Doria, M., Klein, N., Lucito, R. & Schneider, R. J. (1995). The hepatitis B virus HBx protein is a dual specificity cytoplasmic activator of Ras and nuclear activator of transcription factors. *EMBO J* **14**, 4747–4757.

Ganem, D. & Schneider, R. J. (2001). *Hepadnaviridae*: the viruses and their replication. In *Fields Virology*, 4th edn, pp. 2923–2969. Edited by D. M. Knipe, P. M. Howley, D. E. Griffin, R. A. Lamb, M. A. Martin, B. Roizman & S. E. Straus. Philadelphia, PA: Lippincott Williams & Wilkins.

Günther, S., Li, B. C., Miska, S., Kruger, D. H., Meisel, H. & Will, H. (1995). A novel method for efficient amplification of whole hepatitis B virus genomes permits rapid functional analysis and reveals deletion mutants in immunosuppressed patients. *J Virol* **69**, 5437–5444.

Henkler, F., Hoare, J., Waseem, N., Goldin, R. D., McGarvey, M. J., Koshy, R. & King, I. A. (2001). Intracellular localization of the hepatitis B virus HBx protein. *J Gen Virol* **82**, 871–882.

Jacob, J. R., Ascenzi, M. A., Roneker, C. A., Toshkov, I. A., Cote, P. J., Gerin, J. L. & Tennant, B. C. (1997). Hepatic expression of the woodchuck hepatitis virus X-antigen during acute and chronic infection and detection of a woodchuck hepatitis virus X-antigen antibody response. *Hepatology* **26**, 1607–1615.

Keasler, V. V., Hodgson, A. J., Madden, C. R. & Slagle, B. L. (2007). Enhancement of hepatitis B virus replication by the regulatory X protein *in vitro* and *in vivo*. *J Virol* **81**, 2656–2662.

Klein, N. P., Bouchard, M. J., Wang, L. H., Kobarg, C. & Schneider, R. J. (1999). Src kinases involved in hepatitis B virus replication. *EMBO J* **18**, 5019–5027.

Leupin, O., Bontron, S., Schaeffer, C. & Strubin, M. (2005). Hepatitis B virus X protein stimulates viral genome replication via a DDB1-dependent pathway distinct from that leading to cell death. *J Virol* **79**, 4238–4245.

Meier, P., Scougall, C. A., Will, H., Burrell, C. J. & Jilbert, A. R. (2003). A duck hepatitis B virus strain with a knockout mutation in the putative X ORF shows similar infectivity and *in vivo* growth characteristics to wild-type virus. *Virology* **317**, 291–298.

Melegari, M., Wolf, S. K. & Schneider, R. J. (2005). Hepatitis B virus DNA replication is coordinated by core protein serine phosphorylation and HBx expression. *J Virol* **79**, 9810–9820.

Mercer, D. F., Schiller, D. E., Elliott, J. F., Douglas, D. N., Hao, C., Rinfret, A., Addison, W. R., Fischer, K. P., Churchill, T. A. & other authors (2001). Hepatitis C virus replication in mice with chimeric human livers. *Nat Med* **7**, 927–933.

Murakami, S. (2001). Hepatitis B virus X protein: a multifunctional viral regulator. *J Gastroenterol* **36**, 651–660.

Noguchi, C., Ishino, H., Tsuge, M., Fujimoto, Y., Imamura, M., Takahashi, S. & Chayama, K. (2005). G to A hypermutation of hepatitis B virus. *Hepatology* **41**, 626–633.

Ohishi, W., Shirakawa, H., Kawakami, Y., Kimura, S., Kamiyasu, M., Tazuma, S., Nakanishi, T. & Chayama, K. (2004). Identification of rare polymerase variants of hepatitis B virus using a two-stage PCR with peptide nucleic acid clamping. *J Med Virol* **72**, 558–565.

Raney, A. K. & McLachlan, A. (1991). The biology of hepatitis B virus. In *Molecular Biology of the Hepatitis B Virus*, pp. 1–37. Edited by A. McLachlan. Boca Raton, FL: CRC Press.

Seeger, C. & Mason, W. S. (2000). Hepatitis B virus biology. *Microbiol Mol Biol Rev* **64**, 51–68.

Sitterlin, D., Bergametti, F., Tiollais, P., Tennant, B. C. & Transy, C. (2000a). Correct binding of viral X protein to UVDDB-p127 cellular protein is critical for efficient infection by hepatitis B viruses. *Oncogene* **19**, 4427–4431.

Sitterlin, D., Bergametti, F. & Transy, C. (2000b). UVDDB p127-binding modulates activities and intracellular distribution of hepatitis B virus X protein. *Oncogene* **19**, 4417–4426.

Su, Q., Schroder, C. H., Hofmann, W. J., Otto, G., Pichlmayr, R. & Bannasch, P. (1998). Expression of hepatitis B virus X protein in HBV-infected human livers and hepatocellular carcinomas. *Hepatology* **27**, 1109–1120.

Tang, H., Banks, K. E., Anderson, A. L. & McLachlan, A. (2001). Hepatitis B virus transcription and replication. *Drug News Perspect* **14**, 325–334.

Tang, H., Delgermaa, L., Huang, F., Oishi, N., Liu, L., He, F., Zhao, L. & Murakami, S. (2005). The transcriptional transactivation function of HBx protein is important for its augmentation role in hepatitis B virus replication. *J Virol* **79**, 5548–5556.

Tateno, C., Yoshizane, Y., Saito, N., Kataoka, M., Utoh, R., Yamasaki, C., Tachibana, A., Soeno, Y., Asahina, K. & other authors (2004). Near completely humanized liver in mice shows human-type metabolic responses to drugs. *Am J Pathol* **165**, 901–912.

Tsuge, M., Hiraga, N., Takaishi, H., Noguchi, C., Oga, H., Imamura, M., Takahashi, S., Iwao, E., Fujimoto, Y. & other authors (2005). Infection of human hepatocyte chimeric mouse with genetically engineered hepatitis B virus. *Hepatology* **42**, 1046–1054.

Wang, W. L., London, W. T. & Feitelson, M. A. (1991). Hepatitis B X antigen in hepatitis B virus carrier patients with liver cancer. *Cancer Res* **51**, 4971–4977.

Xu, Z., Yen, T. S., Wu, L., Madden, C. R., Tan, W., Slagle, B. L. & Ou, J. H. (2002). Enhancement of hepatitis B virus replication by its X protein in transgenic mice. *J Virol* **76**, 2579–2584.

Yang, P. L., Althage, A., Chung, J. & Chisari, F. V. (2002). Hydrodynamic injection of viral DNA: a mouse model of acute hepatitis B virus infection. *Proc Natl Acad Sci U S A* **99**, 13825–13830.

Zhang, Z., Torii, N., Hu, Z., Jacob, J. & Liang, T. J. (2001). X-deficient woodchuck hepatitis virus mutants behave like attenuated viruses and induce protective immunity *in vivo*. *J Clin Invest* **108**, 1523–1531.

Zoulim, F., Saputelli, J. & Seeger, C. (1994). Woodchuck hepatitis virus X protein is required for viral infection *in vivo*. *J Virol* **68**, 2026–2030.